

Imidazole Aldoximes Effective in Assisting Butyrylcholinesterase Catalysis of Organophosphate Detoxification

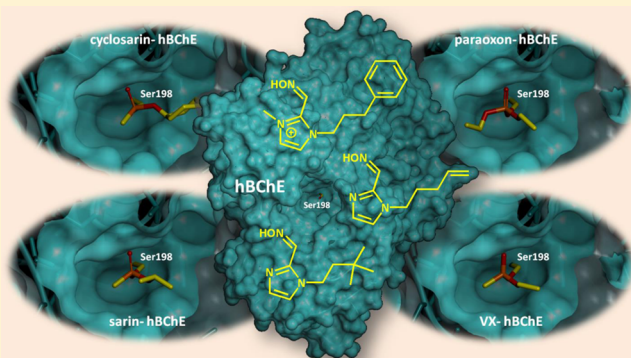
Rakesh K. Sit,[†] Valery V. Fokin,[†] Gabriel Amitai,[‡] K. Barry Sharpless,[†] Palmer Taylor,^{*,§} and Zoran Radic^{*,§}

[†]Skaggs Institute for Chemical Biology and Department of Chemistry, The Scripps Research Institute, La Jolla, California 92037, United States

[‡]Department of Pharmacology, Israel Institute for Biological Research, Ness Ziona 74100, Israel

^{*}Department of Pharmacology, Skaggs School of Pharmacy and Pharmaceutical Sciences, University of California at San Diego, La Jolla, California 92093, United States

ABSTRACT: Intoxication by organophosphate (OP) nerve agents and pesticides should be addressed by efficient, quickly deployable countermeasures such as antidotes reactivating acetylcholinesterase or scavenging the parent OP. We present here synthesis and initial *in vitro* characterization of 14 imidazole aldoximes and their structural refinement into three efficient reactivators of human butyrylcholinesterase (hBChE) inhibited covalently by nerve agent OPs, sarin, cyclosarin, VX, and the OP pesticide metabolite, paraoxon. Rapid reactivation of OP–hBChE conjugates by uncharged and nonprotonated tertiary imidazole aldoximes allows the design of a new OP countermeasure by conversion of hBChE from a stoichiometric to catalytic OP bioscavenger with the prospect of oral bioavailability and central nervous system penetration. The enhanced *in vitro* reactivation efficacy determined for tertiary imidazole aldoximes compared to that of their quaternary *N*-methyl imidazolium analogues is attributed to ion pairing of the cationic imidazolium with Asp 70, altering a reactive alignment of the aldoxime with the phosphorus in the OP–hBChE conjugate.



INTRODUCTION

The recent massive exposure of Syrian citizens to the nerve gas organophosphate (OP) sarin fatally injured hundreds,¹ because of the lack of appropriate antidote intervention. It vividly illustrated an immediate need for effective, affordable, and easily administered countermeasures for rapid protection of large populations from OP exposure. Currently approved antidotal therapies for the treatment of OP poisoning in humans encompass intramuscular injections of pyridinium aldoximes, 2PAM, HI6, obidoxime, toxogonin, or similar agents^{2,3} combined with a muscarinic acetylcholine receptor antagonist (atropine) and an anticonvulsant (benzodiazepine). Alternatively, an intravenously injected highly purified human butyrylcholinesterase (hBChE) can serve as a scavenging agent for the organophosphate in the circulation^{4–7} that is effective both pre- and post-OP exposure.^{7,8}

Pyridinium aldoxime therapy, developed nearly 60 years ago in the seminal work of Wilson and colleagues,⁹ is directed toward nucleophilic reactivation of acetylcholinesterase (AChE) covalently inhibited by OPs to restore catalytic hydrolysis of the neurotransmitter acetylcholine (ACh). Protection by pyridinium aldoximes requires parenteral administration and is limited by their rapid elimination and inability to cross the blood–brain barrier. The OPs are

lipophilic, become sequestered in lipids where they leach from tissues, and thereby allow residual concentrations to persist. Accordingly, antidotal therapy may require repeated administration to sustain appropriate concentrations in target tissues.

Intravenous injection of purified hBChE affords the potential of covalently conjugating the parent OP molecules distributed in the circulation, thus protecting target tissue AChE from OP inhibition. The molecular weight ratio of hBChE to OP forming the OP–hBChE conjugate can be as high as 500–600, so a large mass of BChE is required for it to be an effective scavenger. While proven to be effective in animal studies, stoichiometric scavenging in plasma by hBChE therapy is limited by cost and the practicalities of wider administration to an exposed or potentially exposed population.

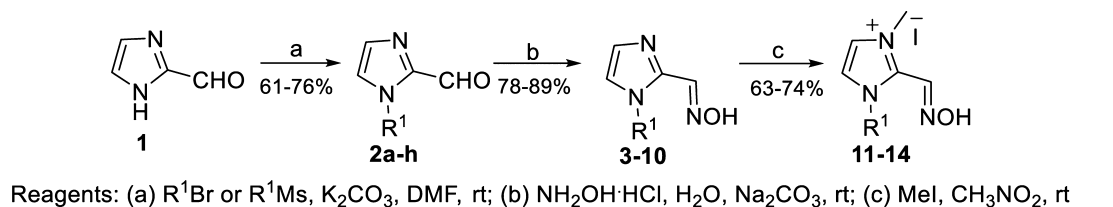
Joint administration of an efficient oxime reactivator of the OP–hBChE conjugate and purified hBChE protein to assist catalysis and turnover of the offending OP in theory should reduce the amount of hBChE needed for efficient protection by establishing a “catalytic bioscavenger” system.¹⁰ We recently demonstrated the feasibility, both *in vitro* and *in vivo*, of a

Received: October 24, 2013

Published: January 28, 2014



Scheme 1



Reagents: (a) R¹Br or R¹Mes, K₂CO₃, DMF, rt; (b) NH₂OH·HCl, H₂O, Na₂CO₃, rt; (c) MeI, CH₃NO₂, rt

3	4	5	6	7	8	9	10
11	12	13	14				

catalytic bioscavenger composed of purified hBChE and a cationic non-pyridinium aldoxime, TAB2OH, with selectivity for BChE reactivation.¹¹ While the catalytic bioscavenger shows a decrease in the size of administered effective hBChE doses, the net protective effects of our catalytic bioscavenger were small because of the relatively low reactivation potency of TAB2OH. Nevertheless, this oxime is to the best of our knowledge the fastest characterized BChE reactuator reported in the literature.

In this study, we follow up on our earlier observation that simple *N*-alkyl imidazole aldoximes can be good reactigators of hBChE¹² and design more effective hBChE reactigators. Although tertiary imidazole-based aldoximes have not been previously described in the literature as cholinesterase reactigators, quaternary imidazolium aldoximes were extensively studied as mono-oxime OP-AChE reactigators^{13–18} and also as bis-oximes in combination with pyridinium and quinuclidinium oximes.^{19–21} Some of these compounds were characterized as promising for reactivation of tabun- and soman-inhibited AChE, both *in vitro* and *in vivo*. Reactivation of OP-inhibited BChE by either tertiary or quaternary imidazole-based aldoximes, on the other hand, had not been described in the literature.

Herein, we thus characterize *in vitro* reactivation properties of a family of uncharged tertiary imidazole aldoximes and their quaternary methylimidazolium analogues against four different OP-hBChE conjugates resulting from sarin, cyclosarin, VX, and paraoxon inhibition of BChE and AChE and show

structural features necessary for efficient OP-hBChE conjugate reactivation. The absence of charge in some of these tertiary imidazole aldoximes bears the promise of reasonable oral bioavailability and retention in tissue as well as potential for central nervous system (CNS) penetration despite some agents having limited solubility. The quaternary analogues are expected to have smaller volumes of distribution and higher initial plasma concentrations.

RESULTS AND DISCUSSION

Chemistry. On the basis of our observation that simple *N*-alkyl-substituted imidazole aldoximes are good reactigators of OP-hBChE conjugates,¹² we synthesized a series of imidazole-2-aldoxime derivatives substituted at N1. This was achieved by alkylation of formylimidazole (1) with the requisite bromide or mesylate, followed by treatment with hydroxylamine as shown in Scheme 1. Using this protocol, a diverse array of aliphatic, aromatic, and unsaturated substituents were incorporated into the N1 position of the imidazole ring (compounds 3–10).

Next, we sought to improve water solubility and nucleophilicity of oxime derivatives via the preparation of quaternary salts by methylating the N3 atom of the imidazole ring. Thus, the quaternization was conducted by reacting selected corresponding mono-oximes with iodomethane to deliver compounds 11–14.

In addition to the 12 imidazole compounds, two cationic mono-oxime derivatives were synthesized. For the preparation of 17 and 18 (Scheme 2), formylimidazole 1 was first reacted

Scheme 2

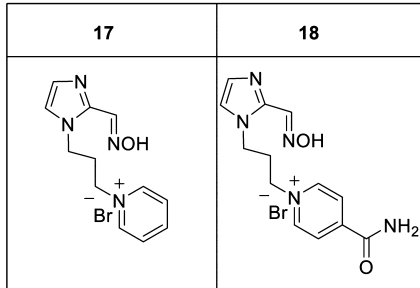
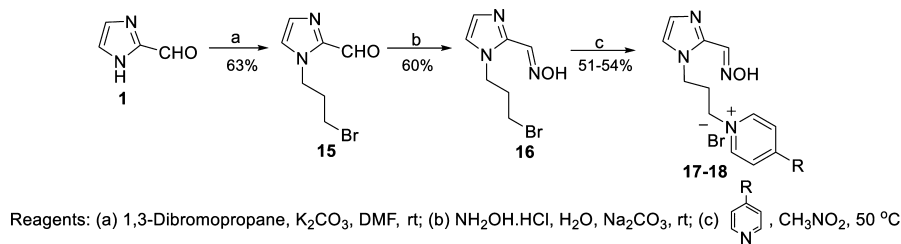


Table 1. Reactivation Rate Constants of 0.67 mM *N*-Alkyl-Substituted Imidazole Aldoximes for OP–hBChE Conjugates Formed by Inhibition of hBChE by Paraoxon and Nonvolatile Analogues of Sarin, Cyclosarin (CS), and VX^a

Oxime	k_{obs} (min ⁻¹)					
	Norm. Avg	POX	Sarin	CS	VX	
RS-115C		75 %	0.029	0.250	0.590	0.370
RS-115B		110 %	0.023	0.680	0.480	0.400
RS-115A		89 %	0.054	0.220	0.650	0.480
RS-113B		160 %	0.190	0.120	0.440	1.200
RS-113A		110 %	0.085	0.180	0.650	0.860
10		53 %	0.0084	0.089	1.030	0.0280

^aThe table shows the dependence of reactivation on the length of the oxime *N*-alkyl chain, for the five RS oximes,¹² and oxime 10. The normalized average (Norm. Avg) k_{obs} was calculated by averaging four k_{obs} values for individual OPs, each expressed as a percentage of the average k_{obs} of all (six in this table) different oximes for that single OP. Experiments were performed at $37\text{ }^\circ C$ in 0.1 M phosphate buffer (pH 7.4) in duplicate.

with 1,3-dibromopropane in *N,N*-dimethylformamide (DMF) using K_2CO_3 as a base while being stirred at room temperature overnight to obtain 1-(3-bromopropyl)-1*H*-imidazole-2-carbaldehyde (**15**). Treatment of **15** with hydroxylamine and Na_2CO_3 at room temperature afforded 1-(3-bromopropyl)-1*H*-imidazole-2-carbaldehyde oxime (**16**). Heating oxime **16**

with pyridine derivatives at $50\text{ }^\circ C$ afforded **17** and isonicotinamide derivative **18**.

Initial Selection of Oxime Structures. Our previously published screen of 135 uncharged oxime reactivators¹² revealed that simple *N*-alkyl-substituted imidazole aldoximes were good reactivators of OP–hBChE conjugates. That study

Table 2. Reactivation Rate Constants of 0.67 mM N-Alkyl-Substituted Imidazole and Imidazolium Aldoximes for OP–hBChE Conjugates Formed by the Inhibition of hBChE by Paraoxon and the Nonvolatile Analogues of Sarin, Cyclosarin (CS), and VX^a

	Oxime	<i>k</i>_{obs} (min⁻¹)				
		Norm. Avrg	POX	Sarin	CS	VX
3		390 %	0.37	0.75	6.0	1.2
4		350 %	0.86	0.31	1.1	3.0
RS-113B		110 %	0.19	0.12	0.44	1.2
5		66 %	0.15	0.15	0.12	0.36
6		67 %	0.049	0.35	0.11	0.10
11		51 %	0.013	0.033	1.6	0.018
17		33 %	0.017	0.057	0.65	0.10
8		15 %	0.016	0.032	0.12	0.095
7		9 %	0.017	0.034	0.023	0.023
18		7 %	0.0030	0.016	0.095	0.030
9		3 %	0.0084	0.0038	0.011	0.015
2PAM		120 %	0.050	0.65	0.29	0.25

^aThe table shows the dependence of reactivation on the substitution at the terminus of the substituted N-alkyl chain. Oximes are ordered by the normalized average (Norm. Avrg) *k*_{obs} (for a description and experimental conditions, see Table 1). Values for 2PAM were not included in the evaluation of the *k*_{obs} average.

was, however, focused on identifying optimal uncharged reactivators of OP–hAChE conjugates; imidazole aldoximes did not surface as optimal candidates. Herein we revisit OP–hBChE conjugate reactivation by imidazole aldoximes and analyze their potencies for reactivation of four individual OP–hBChE conjugates, three identical to those obtained by nerve agent sarin, cyclosarin, and VX inhibition and the fourth obtained by paraoxon inhibition. The nerve agent OP–hBChE conjugates were prepared using Flu-MPs, low-toxicity nerve agent analogues yielding OP–hBChE covalent conjugates identical with the ones formed upon inhibition with nerve agents. The first-order reactivation rate constants at a single

concentration (0.67 mM) of six initial oximes determined under physiological conditions [0.1 M phosphate buffer (pH 7.4) at 37 °C] are listed in Table 1. It appears that the length of the alkyl chain does affect reactivation rates. The N-pentyl derivative RS-113B appeared as the most efficient reactuator of the four conjugates, while shortening or lengthening the alkyl chain oximes generally decreased efficiency. This trend was most evident for VX and paraoxon. Reactivation rate constants for the sarin-derived conjugate peaked at the smaller N-propyl derivative RS-115B, and reactivation of the largest OP–hBChE conjugate, generated by cyclosarin inhibition, was the fastest of all conjugates and for all oximes with a slight preference for the

Table 3. Reactivation Rate Constants of 0.67 mM *N*-Alkyl-Substituted Imidazole and Imidazolium Aldoximes for OP-hBChE Conjugates Formed by the Inhibition of hBChE by Paraoxon and Analogs of Sarin, Cyclosarin (CS), and VX^a

Oxime		<i>K_{obs}</i> (min ⁻¹)				
		Norm. Avrg	POX	Sarin	CS	VX
12		45 %	0.017	0.18	2.5	0.096
14		12 %	0.0049	0.078	0.24	0.059
13		81 %	0.032	0.23	5.7	0.084
3		200 %	0.37	0.75	6.0	1.2
4		220 %	0.86	0.31	1.1	3.0
5		41 %	0.15	0.15	0.12	0.36
2PAM		73 %	0.050	0.65	0.29	0.25
TAB2OH		60 %	0.17	0.087	1.6	0.62
HI6		27 %	0.017	0.15	0.87	0.11
MMB4		15 %	0.021	0.11	0.13	0.056
TMB4		18 %	0.027	0.12	0.17	0.083
obidoxime		22 %	0.025	0.12	0.64	0.069

^aThe table shows the dependence of reactivation on the substitution at the end of the oxime *N*-alkyl chain. For a description of Norm. Avrg and experimental conditions, see Table 1. Values for 2PAM, TAB2OH, HI6, MMB4, TMB4, and obidoxime were not included in the evaluation of the *k_{obs}* average.

longest *N*-alkyl derivative, **10**. Because, of six studied imidazole oximes, the *N*-pentyl imidazole RS-113B appeared to be the most universal efficient reactiver of the four OP-hBChE conjugates, it was selected as a template for further optimization.

Optimization of Oxime Structures. On the basis of the RS-113B structure, seven uncharged and three monocationic mono-oxime derivatives with varying substitutions of the alkyl chain were prepared (Table 2). Their reactivation potencies at a concentration of 0.67 mM were compared to the potencies of

RS-113B and of a very short *N*-alkyl derivative, **9** (Table 2). The simple introduction of a double bond at the end of the *N*-pentyl alkyl chain yielded the most efficient oxime reactiver **3**; it was on average 3-fold faster than RS-113B but particularly efficient for reactivation of cyclosarin, sarin, and VX conjugates of hBChE. Equally efficient was the *N*-dimethylbutyl imidazole **4**; its high efficiency was drastically reduced by elimination of a single methyl to yield **6**. General trends for 13 tested imidazole oximes listed in Table 2 seem to favor a hydrophobic group positioned four methylenes from the imidazole ring. Inserting

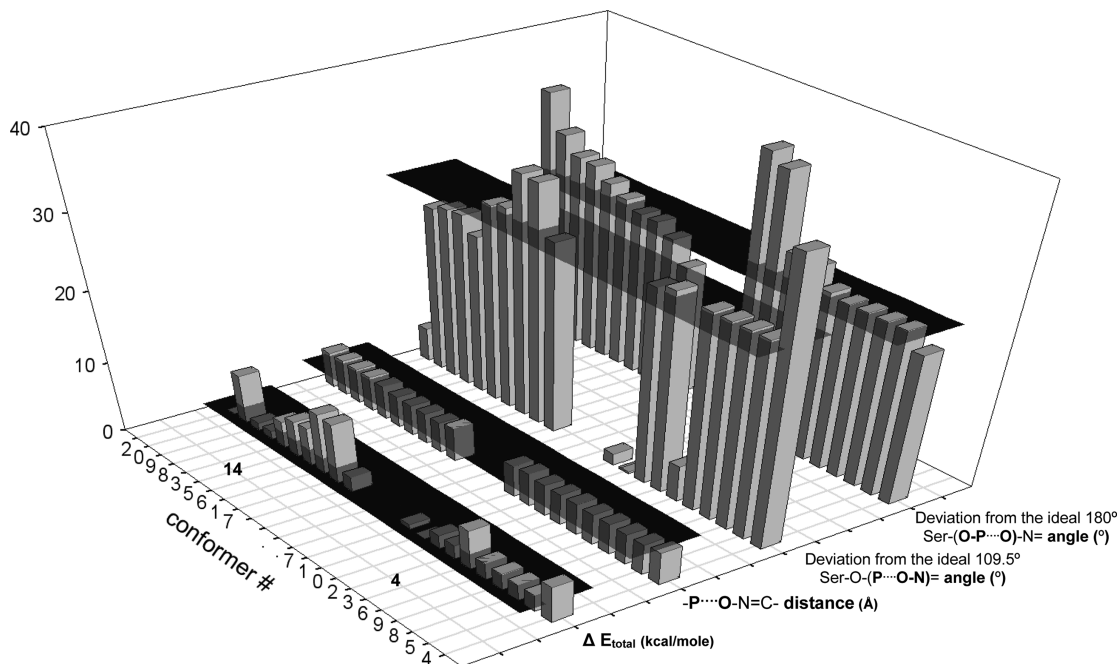


Figure 1. Computational (MD-simulated annealing) analysis of interaction of oximes **4** and **14** in the active center gorge of the VX-hBChE conjugate. For each of two oximes, 10 conformers were calculated and analyzed for their total interaction energies, E_{total} (shown as the difference from the lowest-energy conformer ΔE_{total}), the distance between the nucleophilic oxime O and conjugated phosphorus ($-P\cdots O-N=C-$ distance), and nucleophilic attack angles: Ser-(O-P-O)-N angle (ideally 180°) and Ser-O-(P-O-N)= angle (ideally 109.5°). Horizontal black stripes are shown to emphasize the difference between two oximes.

an azido group to terminate the alkyl chain (compounds **7** and **8**) was counterproductive for reactivation for all OPs. Furthermore, introduction of positive charge generally reduced the reactivation efficacy. For example, quaternization of imidazole into the *N*-methyl imidazolium ring of RS-113B to yield **11** reduced the reactivation efficiency by ~ 1 order of magnitude, except for that of the more bulky cyclosarin conjugate; its reactivation efficiency was enhanced. Introduction of pyridinium in place of a phenyl ring of **5**, to yield **17**, resulted in a similar pattern. Additional small modifications of the pyridinium ring in **17** to yield **18** decreased the reactivation efficiency.

Of the 10 tested RS-113B analogues from Table 2, the two highest-ranking reactivators **3** and **4** were markedly superior for all OP-hBChE conjugate combinations, on average by 4-fold, and significantly better than common reference oximes, 2PAM, HI6, TMB-4, MMB-4, and toxogonin (Table 3).

BChE Reactivation Potencies of Three Selected Imidazole Aldoximes and Their *N*-Methyl Imidazolium Analogues. Along with two highest-ranking reactivators from Table 2 (oximes **3** and **4**), oxime **5** was selected for further structural refinement. Although quaternization of RS-113B, our initial lead from Table 1, had generally negative effects on reactivation potency [conversion of RS-113B into **11** (Table 2)], we decided to prepare and investigate quaternized, imidazolium analogues of **3–5** for several reasons. The first is that imidazolium oximes are expected to be more water-soluble than their tertiary counterparts. Second, quaternization of imidazole nitrogen is expected to change the electronic configuration of the imidazole ring, significantly alter the delocalized system, and reduce the level of protonation of the oxime moiety, thus influencing its nucleophilic reactivity. Finally, reactivation of the cyclosarin OP-hBChE conjugate

was enhanced significantly by the imidazolium analogue of RS-113B [conversion of RS-113B to **11** (Table 2)].

Reactivation rate constants of three imidazolium derivatives along with their tertiary analogues for reactivation of the OP-hBChE conjugate are listed in Table 3. It appears that for only one oxime pair and for only cyclosarin-inhibited hBChE was reactivation enhanced for the quaternary imidazolium, albeit significantly, by ~ 50 -fold [difference between **5** and **13** (Table 3)]. Otherwise, all imidazolium aldoximes exhibited slower reactivation than their tertiary counterparts. More importantly, however, the series of tertiary imidazole compounds were faster reactivators than TAB2OH, to the best of our knowledge the best OP-hBChE conjugate reactuator published to date,¹¹ and in our preliminary *in vivo* experiments less toxic to mice (data not shown). None of the other commonly used pyridinium aldoximes (HI6, MMB4, TMB4, and obidoxime) showed comparable general reactivation potencies for the OP-hBChE conjugates that were tested. The best overall reactuator of all four OP-hBChE conjugates was **4**, being most efficient for the VX-BChE conjugate and several-fold better than any other oxime. Its quaternary analogue, **14**, was on average ~ 70 -fold slower and the slowest of all reactivators in Table 3 for each of four OP-hBChE conjugates.

Modeling the Oxime-BChE Conjugate. Computational molecular modeling of reversible interactions of **4** and **14** within the active center gorge of the VX-hBChE conjugate reveals a higher frequency of reactive oxime orientations for **4** when criteria of lowest interaction energy, shortest distance between oximate oxygen and conjugated OP phosphorus, and smallest deviation from the ideal in-line attack geometry are considered. It appears that for **4** six to seven conformers (#0, #2, #3, #6, #9, #8, and #5, in improving order) of 10 calculated conformers showed comparatively productive properties (Figure 1) and could be matched by only two or three

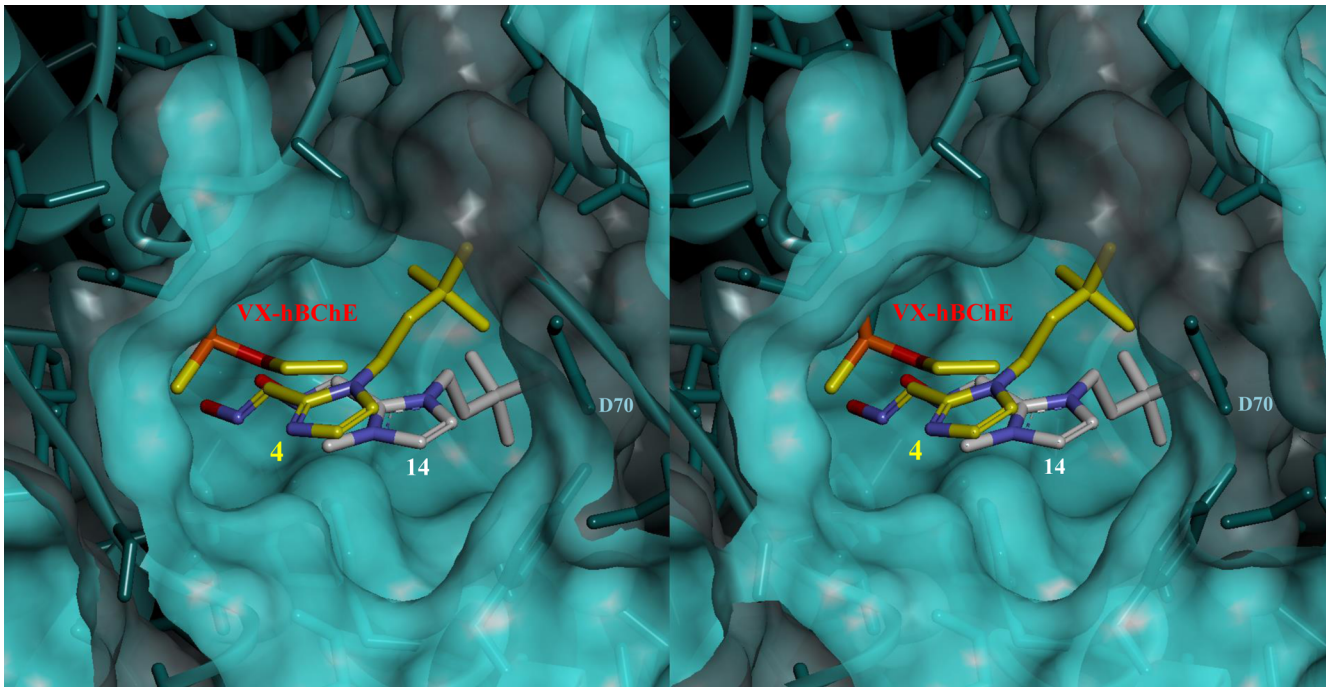


Figure 2. Stereo image of imidazole oximes **4** and **14** docked in the active center gorge of the VX–hBChE conjugate represented by the teal Connolly surface, ribbon, and sticks. Atoms of phosphonyl Ser 198 are represented by sticks (P in orange, C in yellow, and O in red). Oximes are represented by sticks (N in blue, O in red, and C in yellow for **4** and white for **14**). Optimally positioned conformers #7 (**14**) and #5 (**4**) of 10 calculated conformers for each oxime are shown. All imidazolium conformers of **14** were positioned noticeably closer to the anionic aspartate 70 (D70) than tertiary imidazole conformers **4**. Details of computational results are shown in Figure 1.

conformers of **14** (#3, #5, and #7) with similar parameters (Figure 1). Conformers of **14** were consistently found to bind slightly farther from conjugated phosphorus and significantly closer to aspartate 70 of hBChE located in the opposite corner of the hBChE gorge. This is consistent with a Coulombic attraction between the cationic imidazolium ring and anionic Asp 70 of ~4.8 Å that is not possible for the nonprotonated tertiary imidazole derivative **4**, for which the distance was consequently ~6.4 Å (Figure 2). Our preliminary computational analysis thus indicates that this electrostatic interaction may reduce the reactivation efficiency of imidazolium aldoxime **14** by orienting its tertiary butyl side chain deeper into the hydrophobic hBChE gorge (Figure 2).

AChE Reactivation potencies. Reactivation rates of OP-conjugated hAChEs, on the other hand, were relatively slow for all six imidazole aldoximes (Table 4), consistent with the severely restricted size of the OP–hAChE gorge where insertion of hydrophobic side chains of imidazole aldoximes deeper into the gorge likely forces the oximate group into positions farther from conjugated phosphorus. Reactivation rates of imidazoles did not approach those of smaller, cationic 2PAM, except for that of cyclosarin–hAChE conjugate reactivation by imidazolium aldoximes, **12** and **13**, yielding rates comparable to that of 2PAM. Typically, for AChE, imidazolium aldoximes were several-fold slower reactigators than 2PAM and their tertiary analogues even another order of magnitude slower than 2PAM. Thus, unlike reactivation of hBChE, charged imidazolium aldoximes were better reactigators of OP–hAChEs conjugates than tertiary imidazoles (Figure 3). In comparison with TAB2OH, a poor OP–hAChE conjugate reactigator, tertiary imidazoles were similarly poor OP–hAChE conjugate reactigators, but rates were

enhanced by an order of magnitude for quaternary imidazolium reactigators with OP–hAChE conjugates.

Overall Structure–Activity Comparisons. In our previous study,¹¹ we demonstrated both *in vitro* and *in vivo* capacities of TAB2OH, an exocyclic cationic, nonpyridinium aldoxime, to turn over nerve agent OPs catalytically in the presence of purified hBChE. The superior *in vitro* reactivation potency of several imidazole and imidazolium aldoximes against OP–hBChE conjugates, presented in this study in comparison with TAB2OH, positions this series of compounds very favorably for *in vivo* studies of catalytic OP turnover mediated by hBChE. The greater than an order of magnitude enhancement of reactivation rates allows one to consider that reactigators of this general family or its second-generation cousins could become sufficiently efficient *in vivo* to support enhanced OP degradation even in the absence of exogenous administration of purified hBChE. The concentration of naturally occurring hBChE in human plasma is estimated to be ~70 nM,²² and substantial amounts of this enzyme were detected in lung mucosa and intestine, tissue gateways to absorption of initial amounts of toxicant upon nerve gas or pesticide OP exposure.

Furthermore, imidazole aldoximes, as uncharged entities at physiological pH, should be amenable to a more effective distribution across biological membranes resulting in enhanced oral bioavailability compared to those of pyridinium aldoximes. That would allow them to reach OP-exposed tissue rich in BChE and establish catalytic OP degradation *in situ* following a noninvasive oral administration route.

■ CONCLUSION

Imidazole-based aldoximes are identified in this study as a new class of efficient hBChE reactigators. Starting with initial leads

Table 4. Reactivation Rate Constants of 0.67 mM N-Alkyl-Substituted Imidazole and Imidazolium Aldoximes for OP–hAChE Conjugates Prepared and Analyzed As Described in Table 3 for OP–hBChE Conjugates^a

Oxime		<i>k</i>_{obs} (min⁻¹)				
		Norm. Avrg	POX	Sarin	CS	VX
2PAM		5600 %	0.20	0.73	0.067	0.48
TAB2OH		670 %	0.025	0.022	0.0080	0.068
12		180 %	≤ 0.001	0.11	0.073	0.11
14		110 %	≤ 0.001	0.057	0.022	0.099
13		150 %	≤ 0.001	0.11	0.076	0.037
3		68 %	≤ 0.001	0.019	0.026	0.035
4		40 %	≤ 0.001	0.0074	0.0047	0.019
5		54 %	≤ 0.001	0.012	0.012	0.034

^aValues for 2PAM and TAB2OH were not included in the evaluation of the *k*_{obs} average.

identified from our synthetic library, we refined several highly efficient tertiary imidazole and quaternary imidazolium aldoximes to achieve an order of magnitude or more enhancement of *in vitro* OP–hBChE conjugate reactivation rates compared to that of TAB2OH, the most efficient hBChE reactuator published to date. The reduction of a cationic species at physiologic pH values and the prospect of good bioavailability and CNS penetration make tertiary imidazole aldoximes candidates well suited for toxicity, pharmacokinetic, and OP exposure efficacy testing *in vivo*. Thus, we present here a new family of catalytic bioscavengers of nerve agent and pesticide OPs that are dependent on hBChE reactivation. Unlike existing reactigators, these imidazole-based aldoximes have the potential capacity to enlist endogenous tissue hBChE and establish catalytic OP degradation directly in the exposed tissue before lipophilic OPs are distributed into peripheral and central cholinergic innervated target tissues and cause the sequelae of cholinergic hyperexcitation.

EXPERIMENTAL SECTION

Preparation of Novel Oximes. General. All reactions were performed with commercially available ACS grade reagents and solvents. Anhydrous DMF, acetonitrile, and nitromethane were used as received without further purification. All synthesized compounds were determined to possess a purity of more than 95%, as evidenced by high-performance liquid chromatography analysis and ¹H nuclear magnetic resonance (NMR). ¹H NMR and ¹³C NMR spectra were

recorded on a Varian 400 MHz spectrometer. All chemical shifts were reported in parts per million relative to solvent resonances, as indicated (DMSO-*d*₆ δ 2.49, ¹H; δ 39.49, ¹³C) (CDCl₃, δ 7.26, ¹H; δ 77.0, ¹³C). ¹H NMR coupling constants (*J*) are given in hertz.

General Method A for the Preparation of Imidazole Oximes 3–10. To a mixture of formylimidazole 1 and K₂CO₃ in DMF was added the required bromide or mesylate, and the reaction mixture was stirred overnight under an atmosphere of nitrogen at room temperature (rt). The resulting suspension was cooled to rt and filtered. Water was added to the filtrate, and the resulting solution was extracted with Et₂O (3 × 25 mL). The organic layer was dried over MgSO₄ and evaporated to give the corresponding alkylimidazole-2-carbaldehyde.

Hydroxylamine hydrochloride (1.5 equiv) was dissolved in water and neutralized with Na₂CO₃ (1.5 equiv). Alkylimidazole-2-carbaldehyde was added to the solution of hydroxylamine, and the reaction mixture was stirred at rt for 1 h. The resulting precipitate of the corresponding oxime was collected by filtration, rinsed with water, and dried over P₂O₅ under vacuum.

1-(Pent-4-en-1-yl)imidazole-2-carbaldehyde Oxime (3). Prepared according to general method A using formylimidazole 1 (0.50 g, 5.2 mmol), K₂CO₃ (0.72 g, 5.2 mmol), and 5-bromopent-1-ene (0.93 g, 6.2 mmol) in DMF (20 mL). Yellow oil 2a (0.55 g, 64%).

1-(Pent-4-en-1-yl)imidazole-2-carbaldehyde (2a) (0.50 g, 3 mmol), NH₂OH-HCl (0.31 g, 4.5 mmol), water (5 mL), Na₂CO₃ (0.48 g, 4.5 mmol); white solid; yield 0.47 g, 87%; ¹H NMR (400 MHz, DMSO-*d*₆) δ 11.46 (s, 1H), 8.04 (s, 1H), 7.31 (s, 1H), 7.00 (s, 1H), 5.85–5.75 (m, 1H), 5.07–4.94 (m, 2H), 4.23 (t, *J* = 8, 2H), 2.00 (q, *J* = 8, 2H), 1.77 (pent, *J* = 8, 2H); ¹³C NMR (400 MHz, DMSO-*d*₆) δ 141.3,

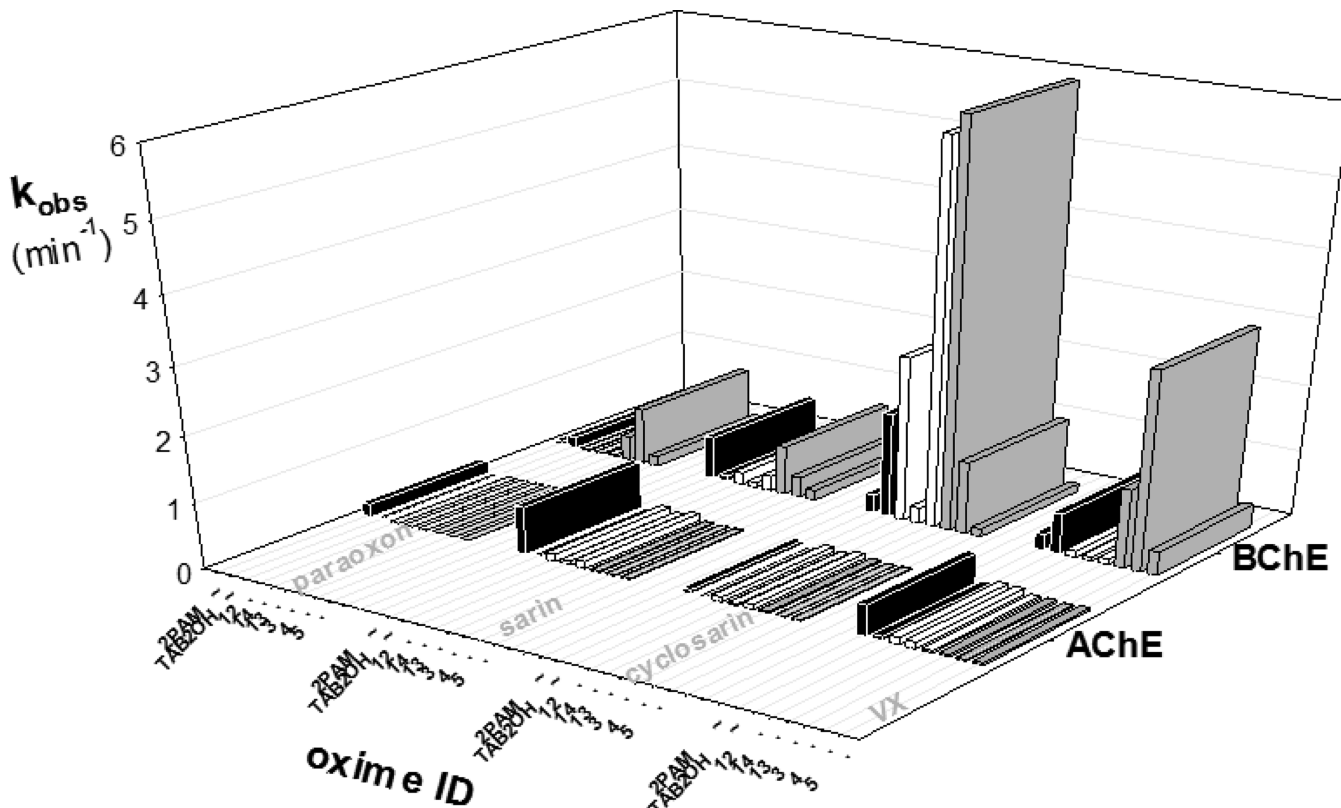


Figure 3. Summary of reactivation rate constants (k_{obs}) of six 0.67 mM *N*-alkyl-substituted imidazole oximes for OP-hAChE and OP-hBChE conjugates formed by inhibition by paraoxon and F1uOP analogues of sarin, cyclosarin, and VX. Gray bars represent data for uncharged tertiary imidazole aldoximes, white bars data for cationic quaternary imidazolium aldoximes, and black bars data for cationic references, pyridinium aldoxime, 2PAM, and nonpyridinium aldoxime, TAB20H. Data are taken from Tables 3 and 4.

139.6, 137.6, 128.8, 123.7, 115.4, 46.2, 30.0, 29.4; LC-MS (ESI) [M + H]⁺ calcd for C₉H₁₄N₃O m/z 180.2, found m/z 180.3.

1-(3,3-Dimethylbutyl)imidazole-2-carbaldehyde Oxime (4). Prepared according to general method A using formylimidazole 1 (0.50 g, 5.2 mmol), K₂CO₃ (0.72 g, 5.2 mmol), and 1-bromo-3,3-dimethylbutane (1 g, 6.2 mmol) in DMF (20 mL). Yellow oil 2b (0.57 g, 61%).

1-(3,3-Dimethylbutyl)imidazole-2-carbaldehyde (2b) (0.54 g, 3 mmol), NH₂OH-HCl (0.31 g, 4.5 mmol), water (5 mL), Na₂CO₃ (0.48 g, 4.5 mmol); white solid; yield 0.52 g, 89%; ¹H NMR (400 MHz, DMSO-*d*₆) δ 11.42 (s, 1H), 8.02 (s, 1H), 7.33 (s, 1H), 6.98 (s, 1H), 4.25 (pent, *J* = 4, 2H), 1.56 (pent, *J* = 4, 2H), 0.93 (s, 9H); ¹³C NMR (400 MHz, DMSO-*d*₆) δ 141.3, 139.4, 128.8, 123.4, 44.3, 43.6, 29.7, 29.2; LC-MS (ESI) [M + H]⁺ calcd for C₁₀H₁₈N₃O m/z 196.3, found m/z 196.3.

1-(3-Phenylpropyl)imidazole-2-carbaldehyde Oxime (5). Prepared according to general method A using formylimidazole 1 (0.50 g, 5.2 mmol), K₂CO₃ (0.72 g, 5.2 mmol), and (3-bromopropyl)-benzene (1.2 g, 6.2 mmol) in DMF (20 mL). Yellow oil 2c (0.77 g, 69%).

1-(3-Phenylpropyl)imidazole-2-carbaldehyde (2c) (0.64 g, 3 mmol), NH₂OH-HCl (0.31 g, 4.5 mmol), water (5 mL), Na₂CO₃ (0.48 g, 4.5 mmol); white solid; yield 0.58 g, 84%; ¹H NMR (400 MHz, DMSO-*d*₆) δ 11.47 (s, 1H), 8.05 (s, 1H), 7.34 (s, 1H), 7.28 (t, *J* = 8, 2H), 7.18 (app d, *J* = 8, 3H), 7.01 (s, 1H), 4.27 (t, *J* = 8, 2H), 2.55 (t, *J* = 8, 2H), 1.99 (pent, *J* = 8, 2H); ¹³C NMR (400 MHz, DMSO-*d*₆) δ 141.3, 141.0, 139.6, 128.8, 128.4, 128.1, 125.9, 123.6, 46.5, 32.0, 31.9; LC-MS (ESI) [M + H]⁺ calcd for C₁₃H₁₆N₃O m/z 230.3, found m/z 230.3.

1-Isopentylimidazole-2-Carbaldehyde Oxime (6). Prepared according to general method A using formylimidazole 1 (0.50 g, 5.2 mmol), K₂CO₃ (0.72 g, 5.2 mmol), and 1-bromo-3-methylbutane (0.94 g, 6.2 mmol) in DMF (20 mL). Yellow oil 2d (0.61 g, 71%).

1-Isopentylimidazole-2-carbaldehyde (2d) (0.50 g, 3 mmol), NH₂OH-HCl (0.31 g, 4.5 mmol), water (5 mL), Na₂CO₃ (0.48 g, 4.5 mmol); white solid; yield 0.44 g, 81%; ¹H NMR (400 MHz, DMSO-*d*₆) δ 11.42 (s, 1H), 8.03 (s, 1H), 7.32 (s, 1H), 6.99 (s, 1H), 4.25 (t, *J* = 8, 2H), 1.59–1.46 (m, 3H), 0.9 (d, *J* = 4, 6H); ¹³C NMR (400 MHz, DMSO-*d*₆) δ 141.4, 139.5, 128.8, 123.5, 45.1, 25.1, 22.3; LC-MS (ESI) [M + H]⁺ calcd for C₉H₁₆N₃O m/z 182.2, found m/z 182.3.

1-(3-Azidopropyl)imidazole-2-carbaldehyde Oxime (7). Prepared according to general method A using formylimidazole 1 (0.50 g, 5.2 mmol), K₂CO₃ (0.72 g, 5.2 mmol), and 3-azidopropylmethanesulfonate (1.1 g, 6.2 mmol) in DMF (20 mL). Yellow oil 2e (0.62 g, 67%).

1-(3-Azidopropyl)imidazole-2-carbaldehyde (2e) (0.54 g, 3 mmol), NH₂OH-HCl (0.31 g, 4.5 mmol), water (5 mL), Na₂CO₃ (0.48 g, 4.5 mmol); white solid; yield 0.46 g, 79%; ¹H NMR (400 MHz, DMSO-*d*₆) δ 11.48 (s, 1H), 8.05 (s, 1H), 7.32 (s, 1H), 7.01 (s, 1H), 4.29 (t, *J* = 8, 2H), 3.33 (t, *J* = 8, 2H), 1.94 (pent, *J* = 8, 2H); ¹³C NMR (400 MHz, DMSO-*d*₆) δ 141.3, 139.6, 128.9, 123.7, 47.9, 44.2, 29.4; LC-MS (ESI) [M + H]⁺ calcd for C₇H₁₁N₆O m/z 195.2, found m/z 195.3.

1-(3-Azidobutyl)imidazole-2-carbaldehyde Oxime (8). Prepared according to general method A using formylimidazole 1 (0.50 g, 5.2 mmol), K₂CO₃ (0.72 g, 5.2 mmol), and 3-azidobutylmethanesulfonate (1.2 g, 6.2 mmol) in DMF (20 mL). Yellow oil 2f (0.68 g, 68%).

1-(3-Azidobutyl)imidazole-2-carbaldehyde (2f) (0.58 g, 3 mmol), NH₂OH-HCl (0.31 g, 4.5 mmol), water (5 mL), Na₂CO₃ (0.48 g, 4.5 mmol); white solid; yield 0.55 g, 88%; ¹H NMR (400 MHz, DMSO-*d*₆) δ 11.54 (s, 1H), 8.06 (s, 1H), 7.33 (s, 1H), 7.02 (s, 1H), 4.26 (t, *J* = 8, 2H), 3.34 (t, *J* = 8, 2H), 1.73 (pent, *J* = 8, 2H), 1.47 (pent, *J* = 8, 2H); ¹³C NMR (400 MHz, DMSO-*d*₆) δ 141.2, 139.5, 128.6, 123.7, 50.2, 46.1, 27.5, 25.3; LC-MS (ESI) [M + H]⁺ calcd for C₈H₁₃N₆O m/z 209.2, found m/z 209.3.

1-(3-Prop-2-yn-1-yl)imidazole-2-carbaldehyde Oxime (9). Prepared according to general method A using formylimidazole 1 (0.50

g, 5.2 mmol), K_2CO_3 (0.72 g, 5.2 mmol), and an 80 wt % propargyl bromide solution in toluene (0.67 mL, 6.2 mmol) in DMF (20 mL). Yellow oil **2g** (0.49 g, 70%).

1-(3-Prop-2-yn-1-yl)imidazole-2-carbaldehyde (2g) (0.40 g, 3 mmol), $NH_2OH\cdot HCl$ (0.31 g, 4.5 mmol), water (5 mL), Na_2CO_3 (0.48 g, 4.5 mmol): white solid; yield 0.35 g, 78%; 1H NMR (400 MHz, DMSO- d_6) δ 11.61 (s, 1H), 8.06 (s, 1H), 7.39 (s, 1H), 7.03 (s, 1H), 5.14 (d, J = 4, 2H), 3.46 (d, J = 4, 2H); ^{13}C NMR (400 MHz, DMSO- d_6) δ 141.0, 139.5, 129.0, 123.2, 78.8, 76.0, 36.5; LC-MS (ESI) [M + H] $^+$ calcd for $C_7H_8N_3O$ m/z 150.2, found m/z 150.3.

1-Nonylimidazole-2-carbaldehyde Oxime (10). Prepared according to general method A using formylimidazole **1** (0.50 g, 5.2 mmol), K_2CO_3 (0.72 g, 5.2 mmol), and 1-bromononane (1.3 g, 6.2 mmol) in DMF (20 mL). Yellow oil **2h** (0.88 g, 76%).

1-Nonylimidazole-2-carbaldehyde (2h) (0.67 g, 3 mmol), $NH_2OH\cdot HCl$ (0.31 g, 4.5 mmol), water (5 mL), Na_2CO_3 (0.48 g, 4.5 mmol): white solid; yield 0.60 g, 84%; 1H NMR (400 MHz, DMSO- d_6) δ 11.44 (s, 1H), 8.03 (s, 1H), 7.30 (s, 1H), 6.98 (s, 1H), 4.21 (d, J = 8, 2H), 1.66 (t, J = 8, 2H), 1.22 (app s, 12H), 0.84 (t, J = 8, 3H); ^{13}C NMR (400 MHz, DMSO- d_6) δ 141.3, 139.5, 128.6, 123.6, 46.6, 31.3, 30.4, 29.0, 28.6, 25.9, 22.1, 13.9; LC-MS (ESI) [M + H] $^+$ calcd for $C_{13}H_{24}N_3O$ m/z 238.3, found m/z 238.4.

General Method B for the Preparation of Imidazole Oximes 11–14. To a solution of iodomethane (0.26 g, 1.8 mmol) in nitromethane (3 mL) was added the corresponding imidazole-2-carbaldehyde oxime (1.5 mmol), and the reaction mixture was stirred overnight at 50 °C. The resulting solution was cooled to rt and concentrated, and water (3 mL) was added. An aqueous solution was extracted with chloroform (2 \times 2 mL). The organic layer was discarded, and the aqueous layer was evaporated. The resulting solid was dried over P_2O_5 under vacuum to give the corresponding imidazole-2-carbaldehyde oxime quaternary salt.

2-[(Hydroxyimino)methyl]-3-methyl-1-pentylimidazol-3-iium Iodide (11). Prepared according to general method B: white solid; yield 0.33 g, 69%; 1H NMR (400 MHz, DMSO- d_6) δ 12.98 (s, 1H), 8.55 (s, 1H), 7.90 (d, J = 4, 1H), 7.85 (d, J = 4, 1H), 4.32 (t, J = 8, 2H), 3.92 (s, 3H), 1.73 (pent, J = 8, 2H), 1.31–1.22 (m, 4H), 0.85 (t, J = 8, 3H); ^{13}C NMR (400 MHz, DMSO- d_6) δ 136.5, 135.5, 124.6, 123.2, 48.7, 36.7, 29.2, 27.6, 21.6, 13.8; LC-MS (ESI) [M] $^+$ calcd for $C_{10}H_{18}N_3O^+$ m/z 196.3, found m/z 196.3. An alternative method for the preparation of this oxime was reported previously.¹⁴

2-[(Hydroxyimino)methyl]-3-methyl-1-(pent-4-en-1-yl)imidazol-3-iium Iodide (12). Prepared according to general method B: white solid; yield 0.36 g, 74%; 1H NMR (400 MHz, DMSO- d_6) δ 12.97 (s, 1H), 8.54 (s, 1H), 7.92 (s, 1H), 7.87 (s, 1H), 5.85–5.75 (m, 1H), 5.05–4.97 (m, 2H), 4.32 (t, J = 8, 2H), 3.92 (s, 3H), 2.05 (q, J = 8, 2H), 1.83 (pent, J = 8, 2H); ^{13}C NMR (400 MHz, DMSO- d_6) δ 137.1, 136.6, 135.4, 124.6, 123.2, 115.6, 48.3, 36.7, 29.6, 28.5; LC-MS (ESI) [M] $^+$ calcd for $C_{10}H_{16}N_3O^+$ m/z 194.3, found m/z 194.3.

2-[(Hydroxyimino)methyl]-3-methyl-1-(3-phenylpropyl)imidazol-3-iium Iodide (13). Prepared according to general method B: white solid; yield 0.35 g, 63%; 1H NMR (400 MHz, DMSO- d_6) δ 13.01 (s, 1H), 8.56 (s, 1H), 7.90 (d, J = 8, 1H), 7.84 (d, J = 8, 1H), 7.29 (t, J = 8, 2H), 7.20 (d, J = 8, 3H), 4.36 (app s, 2H), 3.91 (s, J = 8, 3H), 2.61 (t, J = 8, 2H), 2.06 (pent, J = 8, 2H); ^{13}C NMR (400 MHz, DMSO- d_6) δ 140.6, 136.7, 135.5, 128.4, 128.1, 126.0, 124.7, 123.2, 48.6, 36.7, 31.6, 31.0; LC-MS (ESI) [M] $^+$ calcd for $C_{14}H_{18}N_3O^+$ m/z 244.3, found m/z 244.3.

1-(3-Dimethylbutyl)-2-[(hydroxyimino)methyl]-3-methylimidazol-3-iium Iodide (14). Prepared according to general method B: white solid; yield 0.34 g, 67%; 1H NMR (400 MHz, DMSO- d_6) δ 12.97 (s, 1H), 8.52 (s, 1H), 7.93 (d, J = 4, 1H), 7.83 (d, J = 4, 1H), 4.35 (pent, J = 4, 2H), 3.90 (s, 3H), 1.64 (pent, J = 4, 2H), 0.95 (s, 9H); ^{13}C NMR (400 MHz, DMSO- d_6) δ 136.4, 135.3, 124.6, 123.3, 46.1, 43.1, 40.1, 29.8, 29.0; LC-MS (ESI) [M] $^+$ calcd for $C_{11}H_{20}N_3O^+$ m/z 210.3, found m/z 210.3.

1-(3-Bromopropyl)imidazole-2-carbaldehyde Oxime (16). To a mixture of formylimidazole **1** (3 g, 31.2 mmol) and K_2CO_3 (2.2 g, 15.6 mmol) in DMF (50 mL) was added 1,3-dibromopropane (18.9 g, 93.6 mmol) dropwise, and the reaction mixture was stirred overnight under

a nitrogen atmosphere at rt. Water (120 mL) was added to the resulting suspension, and the solution was extracted with Et_2O (3 \times 50 mL). The organic layer was dried over $MgSO_4$ and evaporated to give 1-(3-bromopropyl)-1*H*-imidazole-2-carbaldehyde (**15**).

Hydroxylamine hydrochloride (3.2 g, 46.8 mmol) was dissolved in water (20 mL) and neutralized with Na_2CO_3 (5 g, 46.8 mmol). 1-(3-Bromopropyl)-1*H*-imidazole-2-carbaldehyde (**15**) was added to the solution of hydroxylamine, and the reaction mixture was stirred at rt for 2 h. The resulting precipitate of the corresponding oxime **16** was filtered out, rinsed with water, and dried over P_2O_5 under vacuum to yield a white solid: yield 4.3 g, 60%; 1H NMR (400 MHz, DMSO- d_6) δ 11.5 (s, 1H), 8.05 (s, 1H), 7.32 (s, 1H), 7.02 (s, 1H), 4.33 (t, J = 8, 2H), 3.44 (t, J = 8, 2H), 2.23 (pent, J = 8, 2H); ^{13}C NMR (400 MHz, DMSO- d_6) δ 141.2, 139.6, 128.9, 123.6, 45.3, 33.0, 31.0; LC-MS (ESI) [M + H] $^+$ calcd for $C_{12}H_{15}N_4O^+$ m/z 231.3, found m/z 231.3; LC-MS (ESI) [M + H] $^+$ calcd for $C_7H_{11}BrN_3O$ m/z 232.1, found m/z 232.1, [M + H + 2] $^+$ m/z 234.1.

General Method C for the Preparation of Imidazole Oximes 17 and 18. To a suspension of imidazole-2-carbaldehyde oxime (**16**) (0.23 g, 1 mmol) in nitromethane (3 mL) was added the corresponding pyridine derivative (1.5 mmol), and the mixture was stirred for 3 days at 50 °C. The resulting solution was cooled to rt and concentrated. Water (3 mL) was added and the mixture washed with chloroform (2 \times 2 mL). The combined organic layers were discarded, and the water layer was evaporated and purified on a reversed-phase biotage using a water/methanol mixture as the eluent. The solvent was evaporated, and the resulting solid was dried over P_2O_5 under vacuum to give the corresponding imidazole-2-carbaldehyde oxime quaternary salt.

1-(3-{2-[(Hydroxyimino)methyl]-1*H*-imidazol-1-yl}propyl)pyridin-1-iium Bromide (17). Prepared according to general method C: brown solid; yield 0.17 g, 54%; 1H NMR (400 MHz, DMSO- d_6) δ 11.46 (s, 1H), 8.05 (s, 1H), 7.33 (s, 1H), 7.27 (t, J = 8, 2H), 7.16 (app d, J = 8, 3H), 7.00 (s, 1H), 4.26 (t, J = 8, 2H), 2.54 (t, J = 8, 2H), 1.98 (pent, J = 8, 2H); ^{13}C NMR (400 MHz, DMSO- d_6) δ 149.9, 149.5, 141.3, 139.6, 128.8, 123.7, 123.6, 46.3, 31.2, 30.5; LC-MS (ESI) [M + H] $^+$ calcd for $C_{12}H_{15}N_4O^+$ m/z 231.3, found m/z 231.3.

4-Carbamoyl-1-(3-{2-[(hydroxyimino)methyl]imidazol-1-yl}propyl)pyridin-1-iium Bromide (18). Prepared according to general method C: brown solid; yield 0.18 g, 51%; 1H NMR (400 MHz, DMSO- d_6) δ 11.52 (s, 1H), 8.60 (s, 1H), 8.08 (s, 1H), 7.84 (2, J = 8, 2H), 7.47–7.31 (m, 4H), 7.07 (s, 1H), 4.39 (t, J = 8, 2H), 4.32 (app s, 2H), 2.34 (app s, 2H); ^{13}C NMR (400 MHz, DMSO- d_6) δ 141.3, 141.0, 139.6, 128.7, 128.3, 128.1, 125.9, 123.5, 46.5, 32.0, 31.9; LC-MS (ESI) [M + H] $^+$ calcd for $C_{13}H_{16}N_5O_2^+$ m/z 274.3, found m/z 274.3.

Enzyme. Highly purified recombinant monomeric hAChE (human AChE) was prepared as described previously.²³ Purified human BChE isolated from human plasma was a gift from D. Lenz and D. Cerasoli [USAMRICD (U.S. Army Medical Research Institute of Chemical Defense), Aberdeen Proving Ground, MD]. All enzyme concentrations given refer to the concentration of catalytic sites, i.e., monomers.

OPs. Low-toxicity nonvolatile Flu-MPs (fluorescent methylphosphonates)²⁴ were used as analogues of nerve agents sarin, cyclosarin, and VX. The Flu-MPs differ from actual nerve agent OPs only by the structure of their respective leaving groups. Inhibition of hBChE and hAChE by Flu-MPs results in OP-hBChE and OP-hAChE covalent conjugates identical with the ones formed upon inhibition with nerve agents. Paraoxon was purchased from Sigma-Aldrich.

Oximes. 2PAM (2-pyridinealdoxime methiodide) and obidoxime [1,1'-(oximidethylene) bis(pyridinium-4-carbaldoxime) dichloride] were purchased from Sigma-Aldrich. TAB2OH and RS-113A, RS-113B, RS-115A, RS-115B, and RS-115C were prepared as described previously.^{11,12} HI6 was purchased from US Biological. MMB4 and TMB4 were gifts from T. Shih and I. Koplowitz (USAMRICD).

Reactivation Assays. hAChE and hBChE activities were measured using a spectrophotometric assay²⁵ at rt in 0.1 M sodium phosphate buffer (pH 7.4), containing 0.01% BSA and 1.0 mM substrate ATCh (acetylthiocholine). OP-hBChE and OP-hAChE

conjugates were prepared using Flu-MPs and paraoxon, and oxime reactivation experiments were performed at 37 °C in 0.1 M sodium phosphate buffer (pH 7.4) containing 0.01% BSA, as described previously.²³ The first-order reactivation rate constant (k_{obs}) for each oxime–OP conjugate combination was calculated by nonlinear regression.²⁶

Computational Molecular Modeling. Molecular models of oximes **4** and **14** were built and prepared using the Insight II modeling suite (Accelrys, San Diego, CA) as described previously for similar aldoximes.²³ The imidazole ring of **4** was not protonated in the calculation, consistent with the determined pK_a of 5.6 (data not shown). The crystal structure of the VX–hBChE conjugate (Protein Data Bank entry 2XQK) was prepared for calculation by removing all water molecules and reversibly bound ligands and repairing incomplete amino acid side chains. Oximes were positioned into the VX–hBChE gorge with their oximate oxygens 4 Å from the conjugated phosphorus atom. A flexible distance constraint was placed between those two atoms at 3 Å, and molecular dynamics (MD) calculations were performed at a series of temperatures starting at 300 K, increasing to 700 K, and decreasing to 300 K in 50 K increments, as described previously for HI6.²³ The structure of hBChE (amide backbone and side chains) was kept fixed because of the relatively large volume of the VX–hBChE gorge, while oxime molecules were allowed to freely rotate. Ten calculations were performed per oxime. Resulting structures were visualized using Discovery Studio Visualizer version 3.5 (Accelrys).

AUTHOR INFORMATION

Corresponding Authors

*E-mail: pwtaylor@ucsd.edu. Phone: (858) 534-1366.

*E-mail: zradic@ucsd.edu. Phone: (858) 534-6841.

Notes

The authors declare no competing financial interest.

ACKNOWLEDGMENTS

The excellent technical assistance of Mrs. Limin Zhang and Ms. Edzna Garcia in reactivation experiments is gratefully acknowledged. This research was supported by the CounterACT Program, National Institutes of Health Office of the Director (NIH OD), and the National Institute of Neurological Disorders and Stroke (Grants U01 NS058046 and R21NS072086).

ABBREVIATIONS

BChE, butyrylcholinesterase; hBChE, human BChE; AChE, acetylcholinesterase; hAChE, human AChE; ATCh, acetylthiocholine; BSA, bovine serum albumin; OP, organophosphate; 2PAM, 2-pyridinealdoxime methiodide

REFERENCES

- Dolgin, E. Syrian gas attack reinforces need for better anti-sarin drugs. *Nat. Med.* **2013**, *19*, 1194–1195.
- Thiermann, H.; Worek, F.; Kehe, K. Limitations and challenges in treatment of acute chemical warfare agent poisoning. *Chem.-Biol. Interact.* **2013**, *206*, 435–443.
- Shih, T. M.; Guarisco, J. A.; Myers, T. M.; Kan, R. K.; McDonough, J. H. The oxime pro-2-PAM provides minimal protection against the CNS effects of the nerve agents sarin, cyclosarin, and VX in guinea pigs. *Toxicol. Mech. Methods* **2011**, *21*, 53–62.
- Cerasoli, D. M.; Griffiths, E. M.; Doctor, B. P.; Saxena, A.; Fedorko, J. M.; Greig, N. H.; Yu, Q. S.; Huang, Y.; Wilgus, H.; Karatzas, C. N.; Koplovitz, I.; Lenz, D. E. In vitro and in vivo characterization of recombinant human butyrylcholinesterase (Protexia) as a potential nerve agent bioscavenger. *Chem.-Biol. Interact.* **2005**, *157*–*158*, 363–365.
- Lenz, D. E.; Yeung, D.; Smith, J. R.; Sweeney, R. E.; Lumley, L. A.; Cerasoli, D. M. Stoichiometric and catalytic scavengers as protection against nerve agent toxicity: A mini review. *Toxicology* **2007**, *233*, 31–39.
- Lockridge, O.; Schopfer, L. M.; Winger, G.; Woods, J. H. Large scale purification of butyrylcholinesterase from human plasma suitable for injection into monkeys; a potential new therapeutic for protection against cocaine and nerve agent toxicity. *Journal of Medical Chemical, Biological and Radiological Defense* **2005**, *3*, nihms5095.
- Güven, M.; Sungur, M.; Eser, B.; Sari, I.; Altuntaş, F. The effects of fresh frozen plasma on cholinesterase levels and outcomes in patients with organophosphate poisoning. *J. Toxicol. Clin. Toxicol.* **2004**, *42*, 617–623.
- Mumford, H. E.; Price, M.; Lenz, D. E.; Cerasoli, D. M. Post-exposure therapy with human butyrylcholinesterase following percutaneous VX challenge in guinea pigs. *Clin. Toxicol.* **2011**, *49*, 287–297.
- Wilson, I. B.; Ginsburg, S. A powerful reactivator of alkylphosphate-inhibited acetylcholinesterase. *Biochim. Biophys. Acta* **1955**, *18*, 168–170.
- Kovarik, Z.; Katalinić, M.; Sinko, G.; Binder, J.; Holas, O.; Jung, Y. S.; Musilova, L.; Jun, D.; Kuča, K. Pseudo-catalytic scavenging: Searching for a suitable reactivator of phosphorylated butyrylcholinesterase. *Chem.-Biol. Interact.* **2010**, *187*, 167–171.
- Radić, Z.; Dale, T.; Kovarik, Z.; Berend, S.; Garcia, E.; Zhang, L.; Amitai, G.; Green, C.; Radić, B.; Duggan, B. M.; Ajami, D.; Rebek, J.; Taylor, P. Catalytic detoxification of nerve agent and pesticide organophosphates by butyrylcholinesterase assisted with non-pyridinium oximes. *Biochem. J.* **2013**, *450*, 231–242.
- Sit, R. K.; Radić, Z.; Gerardi, V.; Zhang, L.; Garcia, E.; Katalinić, M.; Amitai, G.; Kovarik, Z.; Fokin, V. V.; Sharpless, K. B.; Taylor, P. New structural scaffolds for centrally acting oxime reactivators of phosphorylated cholinesterases. *J. Biol. Chem.* **2011**, *286*, 19422–19430.
- Grifantini, M.; Martelli, S.; Stein, M. Structure-activity relationships in reactivators of organophosphorus-inhibited acetylcholinesterase. 5. Quaternary salts of hydroxyiminomethylimidazoles. *J. Pharm. Sci.* **1972**, *61*, 631–633.
- Grifantini, M.; Martelli, S.; Stein, M. Structure-activity relationships in reactivators of organophosphorus-inhibited acetylcholinesterase. 6. 2-Hydroxyiminomethylimidazolium iodides. *J. Med. Chem.* **1973**, *16*, 937–939.
- Bedford, C. D.; Harris, R. N., III; Howd, R. A.; Miller, A.; Nolen, H. W., III; Kenley, R. A. Structure-activity relationships for reactivators of organophosphorus-inhibited acetylcholinesterase: Quaternary salts of 2-[(hydroxyimino)methyl]imidazole. *J. Med. Chem.* **1984**, *27*, 1431–1438.
- Herrador, M. M.; Saénz de Buruaga, J.; Suarez, M. D. Reactivators of organophosphorus-inhibited acetylcholinesterase. 1. Imidazole oxime derivatives. *J. Med. Chem.* **1985**, *28*, 146–149.
- Koolpe, G. A.; Lovejoy, S. M.; Goff, D. A.; Lin, K.-Y.; Leung, D. S.; Bedford, C. D.; Musallam, H. A.; Koplovitz, I.; Harris, R. N. Quaternary salts of 2-[(Hydroxyimino)methyl]imidazole. 5. Structure-activity relationships for side-chain nitro-, sulfone-, amino-, and aminosulfonyl-substituted analogues for therapy against anticholinesterase intoxication. *J. Med. Chem.* **1991**, *34*, 1368–1376.
- Goff, D. A.; Koolpe, G. A.; Kelson, A. B.; Vu, H. M.; Taylor, D. L.; Bedford, C. D.; Musallam, H. A.; Koplovitz, I.; Harris, R. N., III. Quaternary salts of 2-[(hydroxyimino)methyl]imidazole. 4. Effect of various side-chain substituents on therapeutic activity against anticholinesterase intoxication. *J. Med. Chem.* **1991**, *34*, 1363–1368.
- Simeon-Rudolf, V.; Reiner, E.; Skrinjarić-Spoljar, M.; Radić, B.; Lucić, A.; Primožić, I.; Tomić, S. Quinuclidinium-imidazolium compounds: Synthesis, mode of interaction with acetylcholinesterase and effect upon Soman intoxicated mice. *Arch. Toxicol.* **1998**, *72*, 289–295.
- Primožić, I.; Odžak, R.; Tomić, S.; Simeon-Rudolf, V.; Reiner, E. Pyridinium, imidazolium, and quinuclidinium oximes: Synthesis, interaction with native and phosphorylated cholinesterases, and antidotes against organophosphorus compounds. *Journal of Medical*

Chemical, Biological and Radiological Defense **2004**, *2*, http://www.jmedcbr.org/Issue_0201/Reiner_0704.pdf.

(21) Reiner, E.; Simeon, V. Pyridinium, imidazolium and quinuclidinium compounds: Toxicity and antidotal effects against the nerve agents tabun and soman. *Arh. Hig. Rada Toksikol.* **2006**, *57*, 171–179.

(22) Geng, L.; Gao, Y.; Chen, X.; Hou, S.; Zhan, C. G.; Radić, Z.; Parks, R. J.; Russell, S. J.; Pham, L.; Brimijoin, S. Gene transfer of mutant mouse cholinesterase provides high lifetime expression and reduced cocaine responses with no evident toxicity. *PLoS One* **2013**, *8*, e67446.

(23) Cochran, R.; Kalisiak, J.; Kucukkilinc, T.; Radić, Z.; Garcia, E.; Zhang, L.; Ho, K. Y.; Amitai, G.; Kovarik, Z.; Fokin, V. V.; Sharpless, K. B.; Taylor, P. Oxime-assisted acetylcholinesterase catalytic scavengers of organophosphates that resist aging. *J. Biol. Chem.* **2011**, *286*, 29718–29724.

(24) Amitai, G.; Adani, R.; Yacov, G.; Yishay, S.; Teitlboim, S.; Tveria, L.; Limanovich, O.; Kushnir, M.; Meshulam, H. Asymmetric fluorogenic organophosphates for the development of active organophosphate hydrolases with reversed stereoselectivity. *Toxicology* **2007**, *233*, 187–198.

(25) Ellman, G. L.; Courtney, K. D.; Andres, V., Jr.; Featherstone, R. M. A new and rapid colorimetric determination of acetylcholinesterase activity. *Biochem. Pharmacol.* **1961**, *7*, 88–95.

(26) Kovarik, Z.; Radić, Z.; Berman, H. A.; Simeon-Rudolf, V.; Reiner, E.; Taylor, P. Mutant cholinesterases possessing enhanced capacity for reactivation of their phosphorylated conjugates. *Biochemistry* **2004**, *43*, 3222–32229.